The Journal of Immunology

miR-155 Deficiency Ameliorates Autoimmune Inflammation of Systemic Lupus Erythematosus by Targeting *S1pr1* in *Fas*$^{lpr/lpr}$ Mice

Qian Xin, Jiangxia Li, Jie Dang, Xianli Bian, Shan Shan, Jupeng Yuan, Yanyan Qian, Zhaojian Liu, Guangyi Liu, Qianqian Yuan, Na Liu, Xiaochun Ma, Fei Gao, Yaoqin Gong and Qiji Liu

J Immunol 2015; 194:5437-5445; Prepublished online 24 April 2015;
doi: 10.4049/jimmunol.1403028
http://www.jimmunol.org/content/194/11/5437

The Journal of Immunology is published twice each month by
The American Association of Immunologists, Inc.,
9650 Rockville Pike, Bethesda, MD 20814-3994.

Print ISSN: 0022-1767 Online ISSN: 1550-6606.

miR-155 Deficiency Ameliorates Autoimmune Inflammation of Systemic Lupus Erythematosus by Targeting *S1pr1* in *Fas*$^{lpr/lpr}$ Mice

Qian Xin,*,† Jiangxia Li,*,† Jie Dang,*,† Xianli Bian,*,† Shan Shan,*,† Jupeng Yuan,*,† Yanyan Qian,*,† Zhaojian Liu,‡ Guangyi Liu,§ Qianqian Yuan,*,† Na Liu,*,† Xiaochun Ma,*,† Fei Gao,*,† Yaoqin Gong,*,† and Qiji Liu*,†

MicroRNA-155 (miR-155) was previously found involved in the development of systemic lupus erythematosus (SLE) and other autoimmune diseases and the inflammatory response; however, the detailed mechanism of miR-155 in SLE is not fully understood. To explore the in vivo role of miR-155 in the pathogenesis of SLE, miR-155–deficient *Fas*$^{lpr/lpr}$ (miR-155$^{-/-}$*Fas*$^{lpr/lpr}$) mice were obtained by crossing miR-155$^{-/-}$ and *Fas*$^{lpr/lpr}$ mice. Clinical SLE features such as glomerulonephritis, autoantibody levels, and immune system cell populations were compared between miR-155$^{-/-}$*Fas*$^{lpr/lpr}$ and *Fas*$^{lpr/lpr}$ mice. Microarray analysis, RT-PCR, Western blot, and luciferase reporter gene assay were used to identify the target gene of miR-155. miR-155$^{-/-}$*Fas*$^{lpr/lpr}$ mice showed milder SLE clinical features than did *Fas*$^{lpr/lpr}$mice. As compared with *Fas*$^{lpr/lpr}$ mice, miR-155$^{-/-}$*Fas*$^{lpr/lpr}$ mice showed less deposition of total IgA, IgM, and IgG and less infiltration of inflammatory cells in the kidney. Moreover, the serum levels of IL-4 and IL-17a, secreted by Th2 and Th17 cells, were lower in miR-155$^{-/-}$*Fas*$^{lpr/lpr}$ than *Fas*$^{lpr/lpr}$ mice; the CD4^{+}/CD8^{+} T cell ratio was restored in miR-155$^{-/-}$*Fas*$^{lpr/lpr}$ mice as well. Sphingosine-1-phosphate receptor 1 (*S1PR1*) was found as a new target gene of miR-155 by in vitro and in vivo studies; its expression was decreased in SLE patients and *Fas*$^{lpr/lpr}$ mice. miR-155$^{-/-}$*Fas*$^{lpr/lpr}$ mice are resistant to the development of SLE by the regulation of the target gene *S1pr1*. miR-155 might be a new target for therapeutic intervention in SLE. ***The Journal of Immunology*****, 2015, 194: 5437–5445.**

Systemic lupus erythematosus (SLE) (http://www.omim.org/entry/152700) is a typical autoimmune disease characterized by autoantibody production, immune complex deposition, and involvement of multiple organ systems (1). SLE patients show a high serum level of IgM and IgG, and the clinical symptoms are usually accompanied by kidney damage from increased proteinuria level because of the inflammatory cell infiltration.

Immune system dysregulation mediated by immune cells seems to be the main cause of SLE. B cell disorders, including abnormal activation, proliferation, or autoantibody production, are critical reasons for clinical mediation in SLE (2) and have been verified in an SLE mouse model (3). T cells, as well as the proinflammatory cytokines they produce, can promote autoimmune responses in the progression of SLE (4). Recently, many studies showed that Th17 cells expressing IL-17a could mediate the inflammatory response (4). The serum level of IL-17a is increased in SLE patients (5) and the SLE mouse model (6). Although both of these T cell subsets and B cells are regulated by specific microRNAs (miRNAs), the detailed mechanisms of miRNAs controlling the immune cells and whether their targeting can have therapeutic effects are not well known.

miRNAs are a class of endogenous, small noncoding RNAs of 19–22 nt that regulate mRNAs posttranscriptionally (7). By binding to the 3′-untranslated region (UTR) of the target gene mRNA, miRNAs exert their functions by inhibiting elongation, mRNA decay, and mRNA cleavage. Increasing studies have suggested that miRNAs are critical regulators of development and function in the immune system, such as in differentiation of T and B lymphocytes and immune responses (8). Patients and animal models of autoimmune diseases show dysregulated miRNA expression, and functional studies have pinpointed the essential roles of miRNAs in the onset and development of autoimmune diseases such as multiple sclerosis (MS), rheumatoid arthritis (RA), and SLE.

miRNA-155 (miR-155) became a focus in several studies because of its essential functions in autoimmune diseases and inflammatory responses such as MS and RA. Several in vivo and in vitro studies reported that silencing miR-155 could ameliorate the disease severity and delay the onset of experimental autoimmune encephalomyelitis (EAE) and RA (9–12). Additionally, miR-155 was found dysregulated in splenocytes from SLE-prone mice as compared with age-matched controls and was closely related to SLE susceptibility (13).

Therefore, miR-155 might be a proinflammatory factor in immune-related disease, and its deprivation might prevent auto-

*Key Laboratory for Experimental Teratology of the Ministry of Education, Shandong University School of Medicine, Jinan, Shandong 250012, China; †Department of Medical Genetics, Shandong University School of Medicine, Jinan, Shandong 250012, China; ‡Department of Cell Biology, Shandong University School of Medicine, Jinan, Shandong 250012, China; and §Department of Nephrology, Qilu Hospital of Shandong University, Jinan, Shandong 250012, China

Received for publication December 3, 2014. Accepted for publication March 25, 2015.

This work was supported by Natural Science Foundation of China Grants 81072452, 81273281, and 81471602.

The gene expression data presented in this article have been submitted to the Gene Expression Omnibus database under accession number GSE66815.

Address correspondence and reprint requests to Dr. Qiji Liu, Department of Medical Genetics, Shandong University School of Medicine, 44 West Wenhua Road, Jinan, Shandong 250012, China. E-mail address: liuqiji@sdu.edu.cn

The online version of this article contains supplemental material.

Abbreviations used in this article: EAE, experimental autoimmune encephalomyelitis; miR-155, miRNA-155; miRNA, microRNA; MS, multiple sclerosis; PAS, periodic acid–Schiff; PNA, peanut agglutinin; RA, rheumatoid arthritis; SLE, systemic lupus erythematosus; S1P, sphingosine 1-phosphate; S1PR1, sphingosine-1-phosphate receptor 1; Tfh, T follicular helper; UTR, untranslated region; WT, wild-type.

immunity. miR-155 was found overexpressed in the urine of SLE patients but was lower in serum (14, 15). Nonetheless, the study of miR-155 in SLE is still insufficient and little is known about the role of miR-155 in the development of SLE. In the present study, we investigated the role of miR-155 in SLE by generating miR-155$^{-/-}$*Fas*$^{lpr/lpr}$ mice and found that miR-155 deficiency could ameliorate SLE. Furthermore, we found sphingosine-1-phosphate receptor 1 (*S1PR1*) as a target of miR-155 by microarray assay and investigated its expression in patient cells.

Materials and Methods

Patient samples

We enrolled 24 patients with SLE and 34 sex- and age-matched healthy controls from Qilu Hospital of Shandong University at Jinan, China. All SLE patients fulfilled the 1997 American College of Rheumatology revised criteria for SLE. Patients with other diseases or concurrent infection were excluded. Blood samples were obtained from all participants after informed consent. The protocol of this study was approved by the Ethics Review Committee for Human Studies at the School of Medicine, Shandong University.

Generation of miR-155–deficient Fas$^{lpr/lpr}$ *mice and W146 treatment*

Wide-type (WT), *Fas*$^{lpr/lpr}$, and miR-155$^{-/-}$ mice in a C57BL/6 background were purchased from The Jackson Laboratory (Bar Harbor, ME) and maintained under specific pathogen-free conditions. The F_1 generation was generated by crossing *Fas*$^{lpr/lpr}$ and miR-155$^{-/-}$mice, then backcrossing them with *Fas*$^{lpr/lpr}$ mice. Mice homozygous for the lpr mutation and heterozygous for the miR-155 mutation were interbred to maintain the miR-155$^{-/-}$*Fas*$^{lpr/lpr}$ and *Fas*$^{lpr/lpr}$ strains. Mice genotypes of lpr and miR-155 mutation were identified by PCR with DNA obtained by tail biopsy. Mice were sacrificed at the end of life, at ∼10 mo.

Fas was genotyped with the following primer sequences: common, 5′-GTAAATAATTGTGCTTCGTCAG-3′, mutant, 5′-TAGAAAGGTGCACGGGTGTG-3′, and WT, 5′-CAAATCTAGGCATTAACAGTG-3′. miR-155 mouse genotyping primers (WT) were: forward, 5′-GTGCTGCAAACCAGGAAGG-3′, reverse, 5′- CTGGTTGAATCATTGAAGATGG-3′, mutant, 5′- CGGCAAACGACTGTCCTGGCCG-3′. W146 (W1020-1MG, Sigma-Aldrich) was dissolved in DMSO. miR-155$^{-/-}$*Fas*$^{lpr/lpr}$ mice received daily i.p. injections of DMSO or W146 (1 mg/kg) for 3 d and were then sacrificed. All experiments involving animals were approved by the Institutional Animal Care and Use Committee at Shandong University School of Medicine.

Immunostaining of cells and flow cytometry

Abs for mouse CD4-PE, CD8a-PE-Cy7, CD69-FITC, CD45R (B220)-FITC, IgM-PE-Cy7, IgD-PE, CD4-FITC, CD44-PE-Cy7, CXCR5-allophycocyanin, PD-1–PE, and CD138-PE (eBioscience) were used to stain splenocytes or lymph node cells. Suspensions of single splenocytes or lymph node cells were obtained by use of nylon mesh cell strainers (BD Biosciences, C3977-15). Single-cell suspensions were suspended in precooled 1× PBS containing 1% BSA and 0.05% NaN_3. A total of 1×10^5 cells was suspended and stained with sets of conjugated Abs for 20 min on ice. Each sample was washed twice and finally resuspended in 500 μl PBS. Flow cytometry (FACSCanto II, BD Biosciences) involved 50,000 events for each test, with analysis by FlowJo v7.6.5.

Mouse urine collection and proteinuria measurement

Urine from mice 30 wk old or 40–50 wk old was collected for analysis by use of metabolic cages (Hatteras Instruments, MMC100). The proteinuria concentration was detected by Coomassie brilliant blue assay at 595 nm absorbance. Urine collection and measurement was repeated three times.

Isolation of PBMCs

PBMCs were isolated from 3-ml heparinized blood samples of patients and controls by Ficoll gradient centrifugation (Lymphoprep, Nycomed Pharma). Cells from the interphase were collected, washed twice with HBSS (HyClone) and stored in 1 ml TRIzol (Invitrogen) at −80˚C.

RNA extraction and real-time RT-PCR

Total RNA was extracted from cells with use of TRIzol reagent (Invitrogen, 15596-018) following the manufacturer's instructions and treated with RNase-free DNase (Promega, M6101). cDNA was prepared with use of Moloney murine leukemia virus reverse transcriptase (Thermo Scientific, EP0352). Reverse transcriptase involved 2 μg RNA, 1 μl random primers at 65˚C for 10 min, 2 μl dNTP (10 mM), 4 μl 5× buffer, and 1 μl reverse transcriptase. Diethyl pyrocarbonate H_2O was added to 20 μl. Real-time quantitative PCR involved a Roche 480 instrument. Real-time PCR involved 2× FastStart Universal SYBR Green Master mix (Roche, 04913914001), primers (5 μM, 0.5 μl; primer sequences are listed in Supplemental Table I), cDNA (1 μl), and double distilled H_2O (3.5 μl). Four replicates were performed for each reaction: 95˚C for 10 min, 95˚C for 10 s, 60˚C for 20 s, and 60˚C for 30 s for 40 cycles. All samples were run in duplicate, and mRNA was normalized to GAPDH level. The relative mRNA expression was assessed with the $2^{-\Delta\Delta Ct}$ method.

Protein assays

Mouse spleen cells and human PBMCs were lysed by use of TRIzol. Protein was isolated by the TRIzol method. Protein concentration was quantified by the BCA method (Thermo Scientific, 23225). Equal amounts of protein extracts (50 μg) were loaded and separated by 12% SDS-PAGE, electrotransferred to polyvinylidene difluoride membranes, which were incubated with specific primary Abs overnight at 4˚C, and then incubated with HRP-conjugated secondary Abs at room temperature for 1 h and detected by ECL (Thermo Scientific, 32132). Abs for β-actin and S1PR1 were from Epitomics (Burlingame, CA).

Histology, immunohistochemistry, and immunofluorescence

Mice were harvested at age 40 wk. For histology, mouse kidneys were fixed in 4% paraformaldehyde for 24 h at 4˚C, then 0.5% paraformaldehyde for 24 h, and then embedded in paraffin and sectioned. Paraffin tissue sections (5 or 7 μm thick) were stained with H&E or periodic acid–Schiff (PAS). For immunohistochemistry, paraffin renal sections were treated with Ag retrieval solution and permeabilized with 0.2% Triton X-100 in PBS, then blocked before incubation with anti-S1pr1 Ab (Abcam, ab23695). Negative controls were substituting the primary Ab with normal serum. For immunofluorescence, kidneys were immediately frozen to −80˚C in Tissue-Tek OCT compound (Sakura Finetek, 4583). Frozen sections (5 μm thick) were incubated with blocking buffer and stained with FITC-conjugated anti-mouse C1q, IgG, and IgM Abs. Mouse spleen sections were stained with 100 μg/ml peanut agglutinin (PNA; Molecular Probes, L32458) for 30 min, washed three times for 7–8 min with PBS, and observed under the fluorescence microscope after DAPI staining. Slides were analyzed under a laser-scanning confocal microscope.

Cell transfection and luciferase reporter assay

Human embryonic kidney (HEK)293 cells were cultured in DMEM (Life Technologies, 12100-046) supplemented with 10% FBS (HyClone, SH30396.03), 100 U penicillin, and 100 mg/ml streptomycin (Sangon, BS733). Cells were maintained at 37˚C in a humidified atmosphere with 5% CO_2. miR-155 mimics and inhibitors transfection involved use of transfection reagent in 96-well plates (Thermo Fisher Scientific, R0531) according to the manufacturer's instructions. HEK293 cells were harvested after 48 h and lysed by passive lysis buffer. Luciferase activity was measured by the Dual-Luciferase reporter assay system.

ELISA of serum levels of Ig Abs and cytokine

Serum titres of IgG, IgM, and IL-21 were detected in mice by use of an ELISA kit (eBioscience, 88-50400-22, 88-50470, and 88-8210). The mouse Th1-, Th2-, and Th17-related cytokines IFN-γ, IL-4, and IL-17a were detected by use of a cytometric bead array mouse kit for Th1/Th2/Th17 (BD Biosciences, 560485).

Microarray analysis

Mouse spleens were frozen in liquid nitrogen immediately after removal. Total RNA was extracted from WT or miR-155$^{-/-}$ mouse spleens. The amount of RNA from each sample was quantified by use of NanoDrop 1000, and RNA integrity was assessed by standard denaturing agarose gel electrophoresis. Total RNA of each sample was used for labeling and array hybridization as follows: 1) reverse transcription by use of an Invitrogen SuperScript double stranded cDNA synthesis kit; 2) double-stranded cDNA labeling with a NimbleGen one-color DNA labeling kit; 3) array hybridization by the NimbleGen hybridization system and washing with the NimbleGen wash buffer kit; and 4) array scanning with the Axon GenePix 4000B microarray scanner (Molecular Devices). Heat maps were drawn from microarray data.

Statistical analysis

Data analysis involved use of GraphPad Prism (GraphPad Software, San Diego, CA). Quantitative data are expressed as mean ± SD or mean ± SEM.

Differences between two groups were compared by a Student unpaired two-tailed *t* test. A p value <0.05 was considered statistically significant.

Results

miR-155$^{-/-}$Fas$^{lpr/lpr}$ *mice show mild SLE phenotypes*

miR-155 affects immune responses and is involved in the pathology of autoimmune diseases. We found miR-155 overexpressed in the spleen and thymus of *Fas*$^{lpr/lpr}$ mice as compared with WT mice. To investigate whether miR-155 plays a critical role in the development of SLE, miR-155$^{-/-}$*Fas*$^{lpr/lpr}$ mice and their littermates (*Fas*$^{lpr/lpr}$ mice) were obtained by backcrossing and interbreeding. Mice at 40–50 wk old were surveyed for phenotypes. Splenomegaly is a feature of the SLE mouse model (3). Although both miR-155$^{-/-}$*Fas*$^{lpr/lpr}$ mice and *Fas*$^{lpr/lpr}$ mice showed splenomegaly, miR-155$^{-/-}$*Fas*$^{lpr/lpr}$ spleens were significantly smaller than *Fas*$^{lpr/lpr}$ spleens (Fig. 1A). Furthermore, proteinuria level was lower in miR-155$^{-/-}$*Fas*$^{lpr/lpr}$ than *Fas*$^{lpr/lpr}$ mice, with no significant difference between the two genotypes at 30 wk old (Fig. 1B).

To investigate the pathological characteristics in detail, kidney sections of mice were studied by H&E and PAS staining. Although both genotypes showed hyperplasia of the glomerular mesangium, the level was lower for miR-155$^{-/-}$*Fas*$^{lpr/lpr}$ mice (Fig. 1C). Additionally, glomerular enlargement was ameliorated in miR-155$^{-/-}$*Fas*$^{lpr/lpr}$ mice.

Reduced total IgM and IgG titres in serum and immune complex deposition in miR-155$^{-/-}$Fas$^{lpr/lpr}$ *mouse kidney*

Both SLE patients and *Fas*$^{lpr/lpr}$ mice show increased autoantibodies or immune complex deposition in kidneys (16). To further confirm our results, we examined immunofluorescence for IgA, C1q, and IgM in mouse kidney cryosections. Fluorescence intensity was greatly decreased in miR-155$^{-/-}$*Fas*$^{lpr/lpr}$ mice, which suggests reduced immune complex deposition and kidney inflammation (Fig. 2A). Therefore, miR-155$^{-/-}$*Fas*$^{lpr/lpr}$ mice showed reduced disease severity as compared with *Fas*$^{lpr/lpr}$ mice.

Because serum titers of the autoantibodies IgM and IgG are elevated in *Fas*$^{lpr/lpr}$ mice (17), we detected the serum titers of total IgM and IgG induced by B cells. Both IgM and IgG titers were lower in miR-155$^{-/-}$*Fas*$^{lpr/lpr}$ mice than in *Fas*$^{lpr/lpr}$ mice (Fig. 2B).

Reduced percentage of T follicular helper cells and concentration of IL-21 in the miR-155$^{-/-}$Fas$^{lpr/lpr}$ *mouse*

Mouse spleen sections stained with PNA confirmed that there were fewer numbers of spontaneous germinal centers in the miR-155$^{-/-}$*Fas*$^{lpr/lpr}$ spleen compared with the *Fas*$^{lpr/lpr}$ spleen (Fig. 2C). The proportion of Tfh (T follicular helper) cells (CD4$^+$CXCR5$^+$CD44$^+$ PD-1$^+$) was significantly reduced in the miR-155$^{-/-}$*Fas*$^{lpr/lpr}$ mouse lymph nodes. IL-21 is the main cytokine secreted by Tfh cells. ELISA was performed to detect the concentration of IL-21 in mouse serum, and we found that there was a significant reduction of IL-21 in the miR-155$^{-/-}$*Fas*$^{lpr/lpr}$ mice serum compared with *Fas*$^{lpr/lpr}$ mice (Fig. 2D). Additionally, Bcl6 and IL-21 play a critical role in the regulation of Tfh cell differentiation and can be considered as the marker of Tfh cells. We found that *Bcl6* and *IL-21* expression was significantly reduced at the mRNA level in miR-155$^{-/-}$*Fas*$^{lpr/lpr}$ mice spleens (Fig. 2E).

miR-155$^{-/-}$Fas$^{lpr/lpr}$ *mice show a decreased CD4*$^+$*/CD8*$^+$ *cell proportion and active CD4*$^+$ *T cell inflammatory cytokines in miR-155*$^{-/-}$Fas$^{lpr/lpr}$ *serum*

Fas$^{lpr/lpr}$ mice show abnormalities of T and B cells (18). The SLE mouse model is characterized by increased numbers of activated CD4$^+$ T, B, and plasma cells and an increased ratio of CD4$^+$ to CD8$^+$ T cells as compared with WT mice (3). To investigate the cell levels in detail, we examined spleens and lymph nodes by flow cytometry. The proportion of CD4$^+$CD69$^+$cells (Fig. 3A) was decreased ~2-fold in the miR-155$^{-/-}$*Fas*$^{lpr/lpr}$ mouse. miR-155 deficiency could rescue the increased ratio of CD4$^+$ to CD8$^+$ T cells in both spleens and lymph nodes (Fig. 3B). Compared with *Fas*$^{lpr/lpr}$mice, miR-155$^{-/-}$*Fas*$^{lpr/lpr}$ mice showed a significantly greater CD4$^-$CD8$^-$ T cell population (Fig. 3C). B220$^+$, B220$^+$ IgM$^+$, and B220$^+$IgD$^+$ proportions of B cells in spleen did not differ between the genotypes (Fig. 3C).

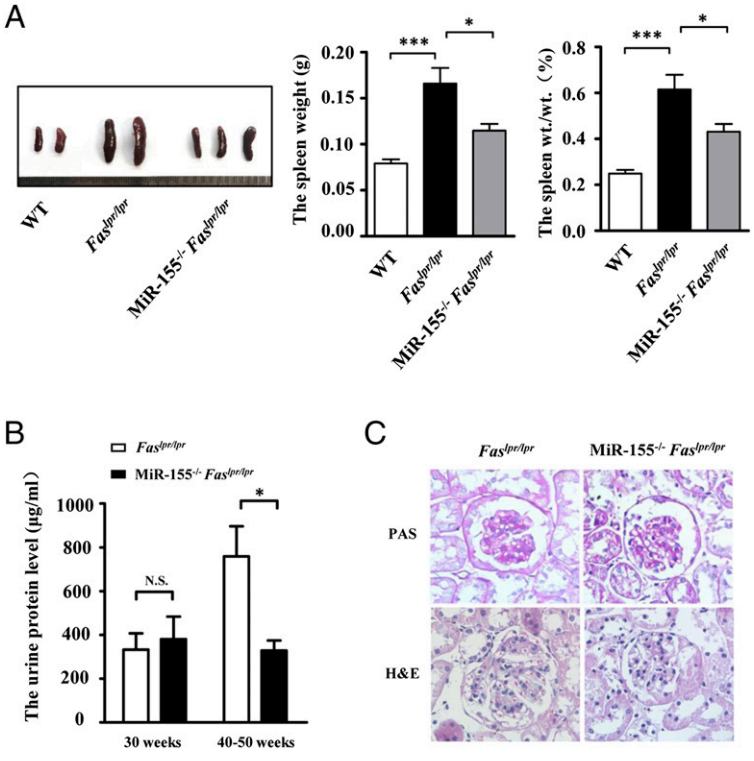

FIGURE 1. Reduced symptoms of lupus-like disease in 40- to 50-wk-old miR-155$^{-/-}$*Fas*$^{lpr/lpr}$ mice. (**A**) Spleens from wild-type (WT), *Fas*$^{lpr/lpr}$, and miR-155$^{-/-}$*Fas*$^{lpr/lpr}$ mice were removed and weight was measured. Representative images of spleens show smaller spleen size of miR-155$^{-/-}$*Fas*$^{lpr/lpr}$ mice than *Fas*$^{lpr/lpr}$ mice (*left*). Spleen weight and the ratio of spleen mass and body mass from WT (n = 7), *Fas*$^{lpr/lpr}$ (n = 11), and miR-155$^{-/-}$*Fas*$^{lpr/lpr}$ (n = 7) mice are shown in the histogram (*right*). (**B**) Proteinuria level quantitatively measured by Coomassie brilliant blue protein assay (n = 8–10). (**C**) Paraffin-embedded sections of mouse kidney were stained with H&E and PAS (original magnification ×200). Representative images are shown. Data were evaluated by a two-tailed unpaired *t* test. Data are mean ± SEM of three independent experiments. *$p < 0.05$, ***$p < 0.001$.

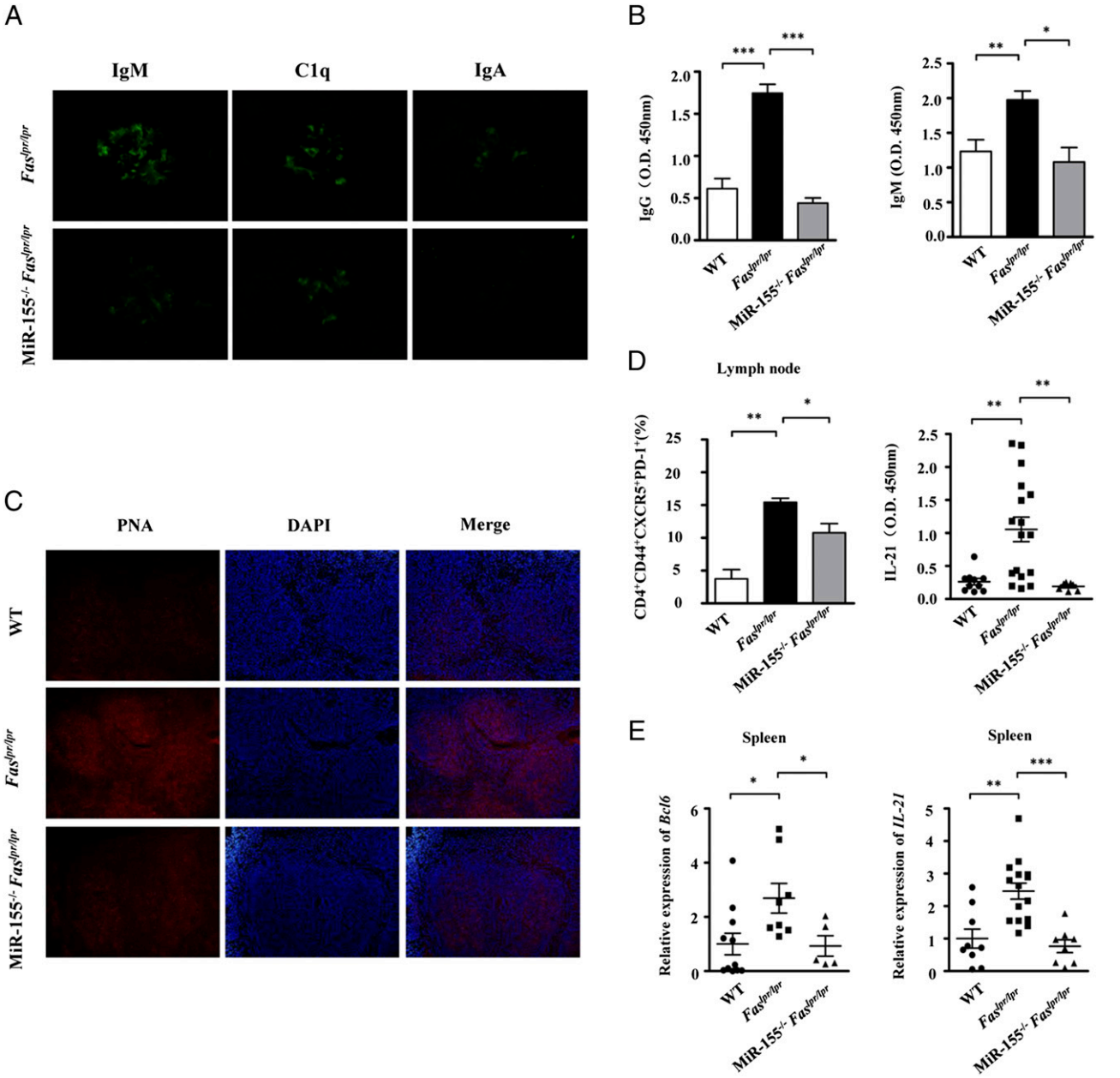

FIGURE 2. Knockout of miR-155 in 40-wk-old $Fas^{lpr/lpr}$ mice reduces autoantibody titers. (**A**) Frozen kidney sections from mice glomeruli were stained with FITC-labeled anti-IgM, C1q, or IgA Ab. Confocal microscopy of representative images are from two independent experiments (original magnification ×200). (**B**) ELISA of titers of total serum IgG and IgM autoantibodies from the indicated mouse strains. (**C**) Representative images of mouse spleen sections of the three mouse strains stained with PNA (Alexa Fluor 568 conjugate) and DAPI (original magnification ×100). (**D**) Flow cytometric analysis of Tfh cell proportion in lymph nodes (n = 5–7) and comparison of concentration of IL-21 in sera of the three mouse strains by ELISA (n = 7–17). (**E**) Quantitative RT-PCR analysis of *Bcl6* and *IL-21* mRNA levels in mouse spleens. Each dot represents an individual mouse (n = 5–15 for each mouse strain). Data are mean ± SD of three independent experiments. $*p < 0.05$, $**p < 0.01$, $***p < 0.001$.

Because aberrant Th cells have been reported in human SLE, we assessed serum levels of the inflammatory cytokines IL-4, IFN-γ, and IL-17a secreted by Th1, Th2, and Th17 cells, respectively, in the mouse. The level of IL-17a and IL-4 was lower in miR-155$^{-/-}$ $Fas^{lpr/lpr}$ than $Fas^{lpr/lpr}$ mice (Fig. 3D). The level of IFN-γ remained the same in the three mouse groups. The absence of miR-155 in $Fas^{lpr/lpr}$ mice may ameliorate the pathological features in part by regulating cell types in SLE.

S1PR1 is negatively regulated by miR-155 in the cell lines and spleen of mice

miRNAs participate in the regulation of mRNA transcription or translation by interacting with the 3′-UTR region of the gene. To determine the target gene of miR-155 in mice, we performed whole-transcriptome analysis of spleens of miR-155$^{-/-}$ and WT mice (accession no. GSE66815, http://www.ncbi.nlm.nih.gov/geo/query/acc.cgi?acc=GSE66815). For genes with >2-fold altered expression, we found 544 upregulated and 508 downregulated genes in miR-155$^{-/-}$ mouse spleens (Fig. 4A). Among the common target genes identified, many are well-established SLE susceptibility genes, such as *Malt1* and *Pxk*. Additionally, genes with altered expression were involved in the immune response and included *Cr2*, *Foxp1*, and *Zeb2*. We confirmed these results by real-time RT-PCR (Fig. 4B).

Venn diagrams were created of upregulated genes detected by whole-transcriptome analysis, as well as targets of miR-155 predicted target genes by miRecords in both mice and humans. The

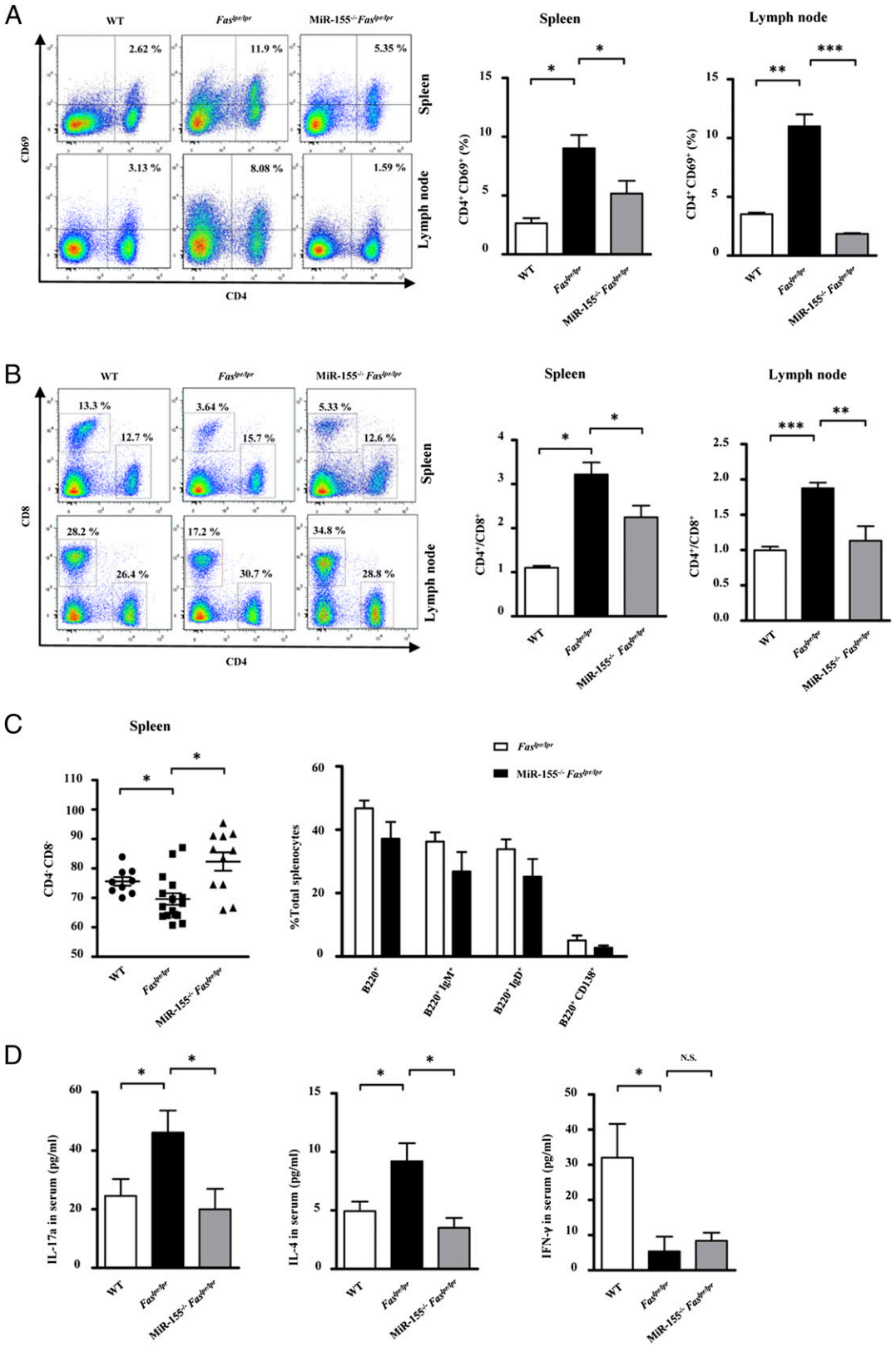

FIGURE 3. Quantitative flow cytometry of cell proportions in spleen or lymph nodes from 40-wk-old WT, $Fas^{lpr/lpr}$, and miR-$155^{-/-}Fas^{lpr/lpr}$ mice. (**A**) Proportion of active $CD4^+$ T ($CD4^+CD69^+$) cells in spleens and lymph node cells. Splenocytes and lymph node cells from 40- to 50-wk-old mice were stained with the indicated Abs and analyzed by flow cytometry. FACS pseudocolor image shows a representative result from three independent experiments (*left*). The histograms show mean active $CD4^+$ T proportion of three groups of mouse spleens and lymph nodes (*right*, $n = 7–9$). (**B**) Ratio of $CD4^+/CD8^+$ in splenocytes and lymph node cells. A representative result shows the ratio of $CD4^+$ and $CD8^+$ cells from spleens and lymph nodes. $CD4^+$ and $CD8^+$ T cell in spleens and lymph nodes are circled in the FACS pseudocolor image (*left*).The statistical results of $CD4^+/CD8^+$are shown in the histograms (*right*, $n = 7–9$) (**C**) Proportion of $CD4^-CD8^-$ cells and B cells subsets in mouse spleens. Each symbol represents an individual mouse (*left*). Splenocytes were labeled with B220, IgM, IgD, and CD138 Abs for subsets of $B220^+$and $B220^+IgM^+$, $B220^+IgD^+$, and $B220^+CD138^+$ cells (*right*, $n = 8–12$). (**D**) Serum levels of T cell–related cytokines IL-4, IL-6, and IFN-γ. Data are mean ± SD of three independent experiments. $*p < 0.05$, $**p < 0.01$, $***p < 0.001$.

union of three sets contains *Satb1*, *H3f3a*, *Sla*, and *S1pr1* in the Venn analysis (Fig. 4C). *S1PR1*, which participates in immune inflammatory responses, was predicted using four commonly used software. As shown in Fig. 4D, the 3′-UTR region of *S1PR1* may serve as binding site for miR-155 in humans and mice.

To further confirm that *S1PR1* is indeed a target gene of miR-155, we used luciferase assay and transfection experiments. pmirGlo vectors including the *S1PR1* 3′-UTR sequence and miR-155–specific mimics or inhibitors were cotransfected into HEK293 cells for Dual-Luciferase activity assay. Luciferase ac-

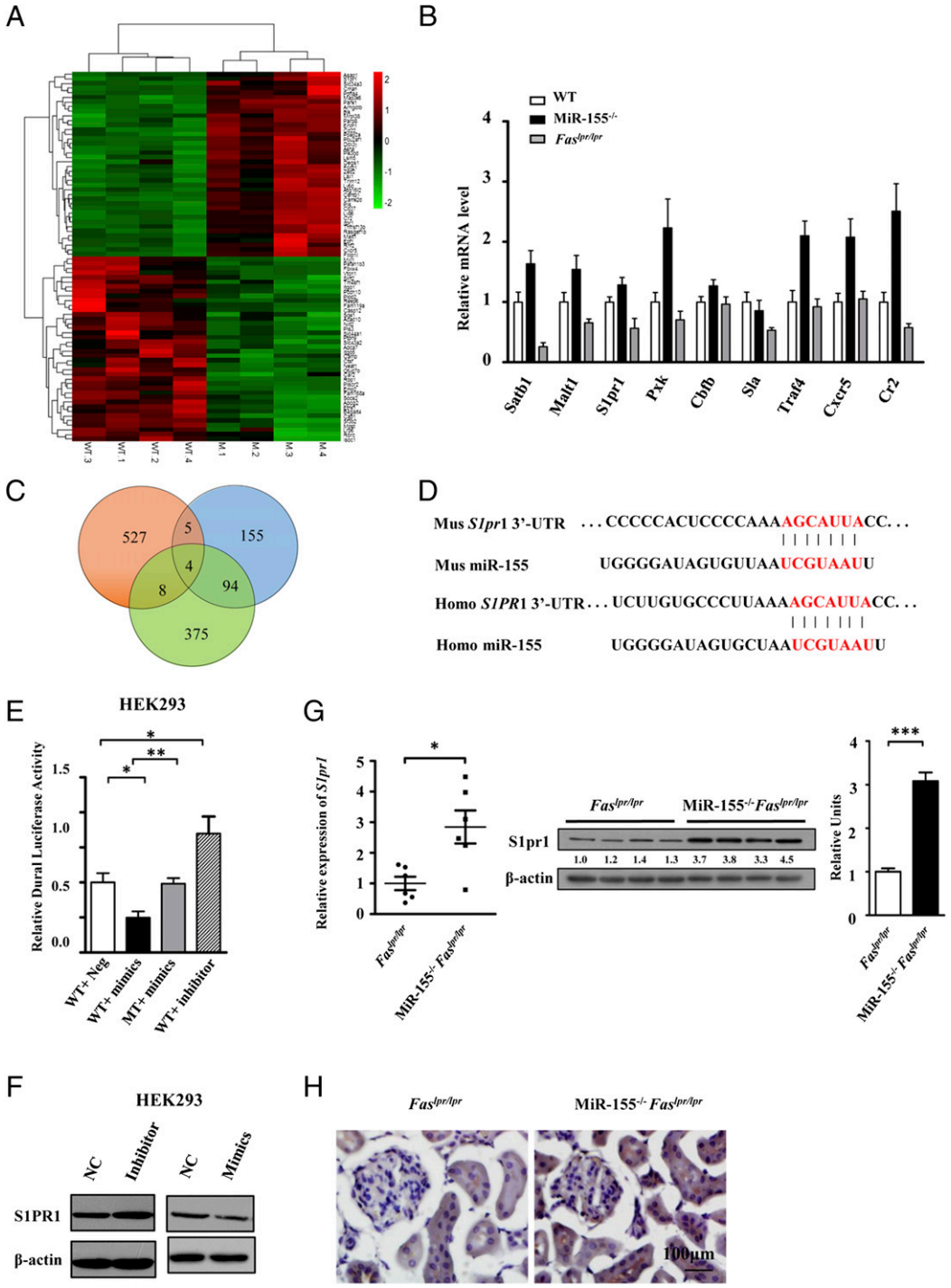

FIGURE 4. Microarray assay of gene expression patterns in spleens of WT and miR-155$^{-/-}$ mice and the verification of decreased S1PR1 expression by miR-155 through binding to the 3′-UTR region. (**A**) Heat map of representative genes with change in expression >2-fold difference at $p < 0.05$ in spleens. Red or green indicates relative high or low expression levels, respectively ($n = 4$). (**B**) Quantitative RT-PCR verification of chip results ($n = 8$–10 for each mouse strain). Relative fold changes for each gene were set to 1 for WT mice. Data are mean ± SD from three independent biological replicates (experimental error). (**C**) Venn analysis of chip results (red), predictive human targets (green), and mouse target genes (blue) of miR-155. (**D**) Schematic view of human and mouse miR-155 binding site of *S1PR1*. Red shows the seed sequence of miR-155. Vertical lines indicate Watson–Crick and wobble base pairing, respectively. (**E**) Luciferase reporter assay of HEK293 cells with WT or mutant 3′-UTR vector and contransfected with mimics or inhibitor of miR-155. (**F**) Western blot analysis of S1PR1 in HEK293 cells transiently transfected with miR-155 mimics or inhibitors for 48 h. NC, normal control. (**G**) RT-PCR and Western blot analysis and quantification of mRNA and protein levels, respectively, of S1PR1. Band intensity is underneath the gel image. (**H**) Representative immunohistochemical staining of S1pr1 using hematoxylin in kidneys of *Fas*$^{lpr/lpr}$ and miR-155$^{-/-}$*Fas*$^{lpr/lpr}$ mice. Data are mean ± SD from three independent experiments. *$p < 0.05$, **$p < 0.01$, ***$p < 0.001$.

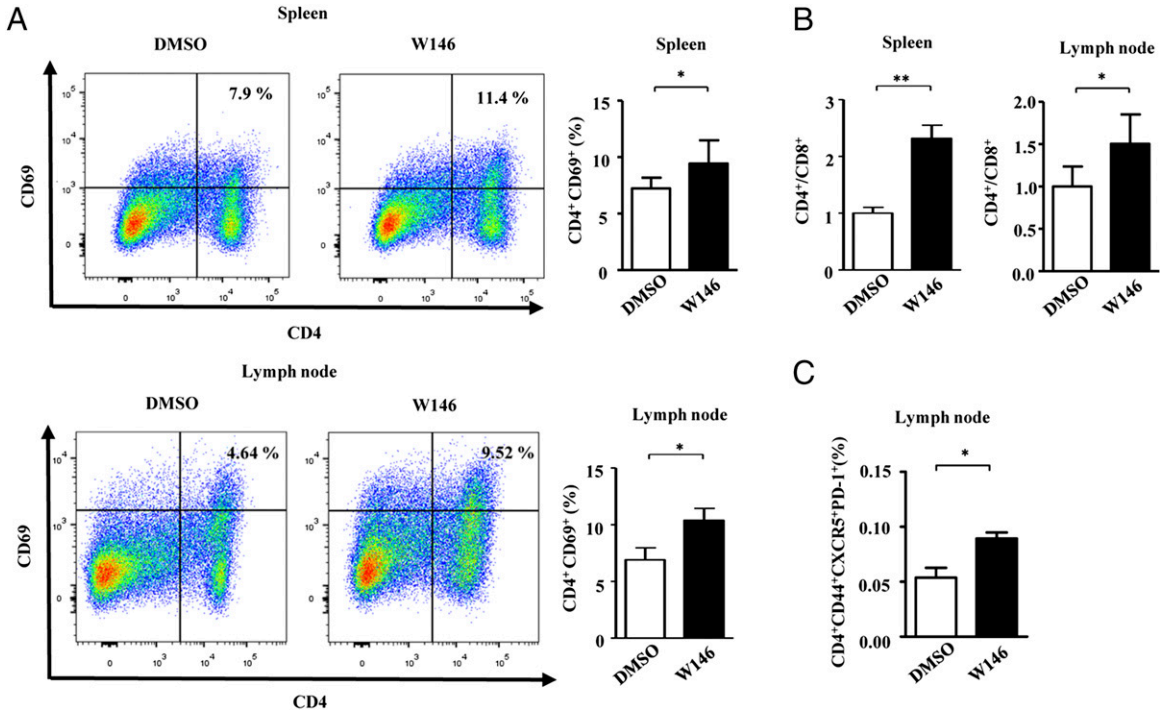

FIGURE 5. Increased proportion of activated CD4 cells and $CD4^+/CD8^+$ T cells in spleens and Tfh cells in the lymph nodes in W146-treated miR-$155^{-/-}Fas^{lpr/lpr}$ mice. (**A**) Proportion of active $CD4^+$ ($CD4^+CD69^+$) T cells in splenocytes and lymph node cells from DMSO- and W146-treated miR-$155^{-/-}Fas^{lpr/lpr}$ mice. FACS pseudocolor image shows a representative result from three independent experiments (*left*). The histograms show mean active $CD4^+$ T proportion of two groups of mouse spleens and lymph nodes (*right*, $n = 5–7$). (**B**) Ratio of $CD4^+/CD8^+$ in mouse splenocytes and lymph node cells ($n = 5–7$). (**C**) Proportion of Tfh cells in lymph node cells ($n = 5–7$). Data are mean ± SD of three independent experiments. $*p < 0.05$, $**p < 0.01$.

tivity was decreased as compared with the control, so miR-155 may interact with the *S1PR1* 3′-UTR and then inhibit gene expression. Luciferase activity was not affected by mutant vector transfection (Fig. 4E). miR-155 inhibitor transfected in HEK293 cells downregulated miR-155 activity and increased the expression of S1PR1. However, when HEK293 cells were transfected with miR-155 mimics, the expression of S1PR1 was decreased (Fig. 4F). In vivo, *S1PR1* mRNA and protein levels were upregulated 3-fold in the spleen of miR-155–deficient $Fas^{lpr/lpr}$ mice (Fig. 4G). The increased expression of S1PR1 was detected in

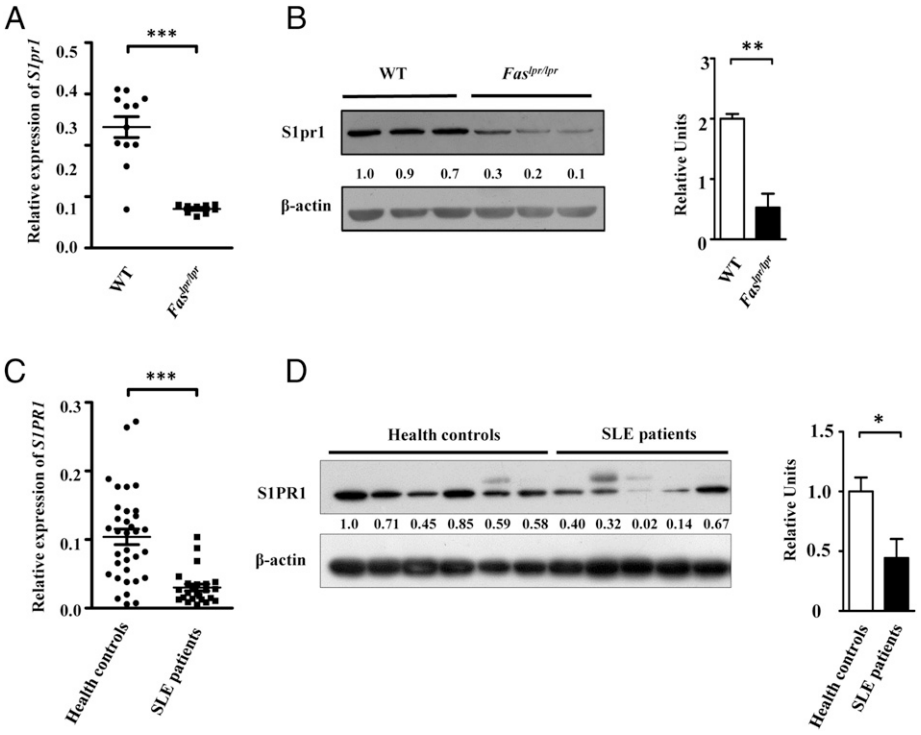

FIGURE 6. S1PR1 is downregulated in mice spleen and SLE patient PBMCs. Quantitative RT-PCR analysis of mRNA level (**A**) and Western blot analysis and quantification of protein level (**B**) of S1pr1 in spleens of mice. Expression is relative to β-actin level (B). (**C** and **D**) Level of S1PR1 in PBMCs from SLE patients and healthy controls (C) and Western blot analysis and quantification of protein level (D). Levels are relative to those of β-actin. Each experiment was repeated at least three times. Data are mean ± SEM. $*p < 0.05$, $**p < 0.01$, $***p < 0.001$.

miR-155$^{-/-}$*Fas*$^{lpr/lpr}$ mouse kidneys (Fig. 4H). In summary, *S1PR1* is a target gene of miR-155, and miR-155 regulates its expression at the posttranscriptional level.

S1PR1-*specific antagonist W146 could accelerate inflammatory phenotypes of miR-155*$^{-/-}$Fas$^{lpr/lpr}$ *mice*

We have confirmed that miR-155 could negatively regulate S1PR1 expression in vitro. Next, we explored whether miR-155 is involved in the development of SLE by regulating *S1PR1* in vivo. W146 is a specific antagonist S1PR1. miR-155$^{-/-}$*Fas*$^{lpr/lpr}$ mice were received daily i.p. injections of DMSO or W146 (1 mg/kg). Mice were sacrificed after 3 d and the proportions of cell subtypes were detected. We found that the proportion of activated CD4$^+$ T was increased in the W146-treated mice lymph nodes and spleens (Fig. 5A). Moreover, the ratio of CD4$^+$/CD8$^+$ was also increased (Fig. 5B). Additionally, the proportion of Tfh cell was also increased in lymph nodes of W146-treated mice compared with DMSO-treated mice (Fig. 5C). Overall, miR-155 was involved in development of SLE by regulating the expression of S1pr1 in vivo.

S1PR1 is downregulated in PBMCs of SLE patients and splenocytes of Fas$^{lpr/lpr}$ *mice*

To confirm whether S1PR1 is involved in the pathogenesis of SLE, we explored S1PR1 expression in human PBMCs from SLE patients and *Fas*$^{lpr/lpr}$ mouse splenocytes. As expected, S1pr1 mRNA and protein expression was decreased in *Fas*$^{lpr/lpr}$ mouse splenocytes and patient PBMCs (Fig. 6).

Discussion

In this study, we investigated the role of miR-155 in the pathogenesis of SLE using a knockout mouse model in vivo. miR-155 deficiency could reduce disease severity and ameliorate the lupus-like phenotypes of the *Fas*$^{lpr/lpr}$ mouse. Moreover, total serum levels of IgM and IgG and immune complex deposition in the mouse kidney were decreased in miR-155$^{-/-}$*Fas*$^{lpr/lpr}$ mice. *S1PR1* is a target of miR-155, and its mRNA and protein expression was increased in PBMCs from SLE patients and *Fas*$^{lpr/lpr}$ mouse splenocytes.

miR-155 is located at 21q21.3, the B cell integration cluster, originally considered to be a proto-oncogene associated with lymphoma. miR-155 was implicated in the innate immune function from evidence of dysregulated miR-155 in many autoimmune diseases, which demonstrated that miR-155 was pivotal for the immune and inflammatory response (9, 19–21). miR-155 was found to promote the development of EAE, an established mouse model of MS (9). The expression of miR-155 was elevated in the synovial membrane and synovial fluid macrophages from patients with RA (10). Furthermore, miR-155–deficient mice did not exhibit collagen-induced arthritis (10, 11).

In the EAE model, miR-155–deficient mice demonstrated abnormal proportion and function of immune cells, especially Th1 and Th17 cells (21). Additionally, miR-155–deficient mice showed reduced numbers of T regulatory cells, so miR-155 might promote the development of T regulatory cells (22). Additionally, miR-155 could regulate the germinal center response of B cells, and deprivation of miR-155 in B cells could reduce the secreted IgG1 Ab (23). miR-155–deficient B cells cannot generate reduced extrafollicular and germinal center responses and secrete high-affinity IgG1 Abs (23). Deletion of miR-155 was found to alleviate lupus-like disease in the *Fas*$^{lpr/lpr}$ mouse (24). Therefore, miR-155 plays an important role in the pathogenesis of SLE.

Several studies identified many direct target genes of miR-155. miR-155 could downregulate suppressor of cytokine signaling 1 (25) and src homology 2 domain-containing inositol-5-phosphatase 1 (26) and then play a critical function in the immune response. Additionally, miR-155 promoted Ig class switching in B cells by targeting the transcription factor PU.1 (27). Our in vivo and in vitro studies indicated that *S1PR1* is a new target gene of miR-155. *S1PR1*, a G protein–coupled receptor, can bind to the bioactive signaling molecule S1P for a critical role in the regulation of lymphocyte maturation, migration, and trafficking. Additionally, S1PR1 and S1P signaling is essential for autoimmune diseases such as MS and RA and the inflammatory responses (28, 29).

Although studies of S1PR1 in SLE have been rarely reported, increasing evidence suggests that S1PR1 might be involved in the pathogenesis of SLE. Microarray analysis of Th17 cells from SLE patients showed decreased mRNA level of *S1PR1* (30). Fingolimod (FYT720), an analog of sphingosine, which functions as an immunosuppressant, is an effective drug used to treat MS (31). Phosphorylated fingolimod promotes the internalization of S1PR1 and then stops the lymphocytes moving from lymph nodes to peripheral tissues (32). Thus, we next investigated what role, if any, S1PR1 plays in the pathogenesis of SLE. Both the mRNA and protein levels of S1PR1 were decreased more in SLE patients than in healthy controls. Consistent results were obtained in the spleens of *Fas*$^{lpr/lpr}$ mice and littermates. Thus, the expression of S1PR1 might be correlated with the pathogenesis of SLE, and the factor might be a potential therapeutic target for the treatment of SLE. All of these data provide solid evidence for the role of *S1PR1* in SLE pathogenesis and development. Further investigations to understand the detailed mechanisms of S1PR1 in SLE are required.

In conclusion, we demonstrated that miR-155–deficient *Fas*$^{lpr/lpr}$ mice are strongly protected against the development of SLE lesions. How this occurs might depend in part on its new target gene *S1PR1*. miR-155 may be a valid therapeutic target in the treatment of SLE.

Acknowledgments

We thank Dr. Hong Li for help in renal pathology analysis.

Disclosures

The authors have no financial conflicts of interest.

References

1. Wakeland, E. K., K. Liu, R. R. Graham, and T. W. Behrens. 2001. Delineating the genetic basis of systemic lupus erythematosus. *Immunity* 15: 397–408.
2. Sanz, I., and F. E. Lee. 2010. B cells as therapeutic targets in SLE. *Nat Rev Rheumatol* 6: 326–337.
3. Mohan, C., L. Morel, P. Yang, H. Watanabe, B. Croker, G. Gilkeson, and E. K. Wakeland. 1999. Genetic dissection of lupus pathogenesis: a recipe for nephrophilic autoantibodies. *J. Clin. Invest.* 103: 1685–1695.
4. Crispín, J. C., M. Oukka, G. Bayliss, R. A. Cohen, C. A. Van Beek, I. E. Stillman, V. C. Kyttaris, Y. T. Juang, and G. C. Tsokos. 2008. Expanded double negative T cells in patients with systemic lupus erythematosus produce IL-17 and infiltrate the kidneys. *J. Immunol.* 181: 8761–8766.
5. Wong, C. K., L. C. Lit, L. S. Tam, E. K. Li, P. T. Wong, and C. W. Lam. 2008. Hyperproduction of IL-23 and IL-17 in patients with systemic lupus erythematosus: implications for Th17-mediated inflammation in auto-immunity. *Clin. Immunol.* 127: 385–393.
6. Zhang, Z., V. C. Kyttaris, and G. C. Tsokos. 2009. The role of IL-23/IL-17 axis in lupus nephritis. *J. Immunol.* 183: 3160–3169.
7. Bartel, D. P. 2004. MicroRNAs: genomics, biogenesis, mechanism, and function. *Cell* 116: 281–297.
8. Baltimore, D., M. P. Boldin, R. M. O'Connell, D. S. Rao, and K. D. Taganov. 2008. MicroRNAs: new regulators of immune cell development and function. *Nat. Immunol.* 9: 839–845.
9. Murugaiyan, G., V. Beynon, A. Mittal, N. Joller, and H. L. Weiner. 2011. Silencing microRNA-155 ameliorates experimental autoimmune encephalomyelitis. *J. Immunol.* 187: 2213–2221.
10. Kurowska-Stolarska, M., S. Alivernini, L. E. Ballantine, D. L. Asquith, N. L. Millar, D. S. Gilchrist, J. Reilly, M. Ierna, A. R. Fraser, B. Stolarski, et al. 2011. MicroRNA-155 as a proinflammatory regulator in clinical and experimental arthritis. *Proc. Natl. Acad. Sci. USA* 108: 11193–11198.
11. Blüml, S., M. Bonelli, B. Niederreiter, A. Puchner, G. Mayr, S. Hayer, M. I. Koenders, W. B. van den Berg, J. Smolen, and K. Redlich. 2011. Essential

role of microRNA-155 in the pathogenesis of autoimmune arthritis in mice. *Arthritis Rheum.* 63: 1281–1288.
12. Jin, H. M., T. J. Kim, J. H. Choi, M. J. Kim, Y. N. Cho, K. I. Nam, S. J. Kee, J. B. Moon, S. Y. Choi, D. J. Park, et al. 2014. MicroRNA-155 as a proinflammatory regulator via SHIP-1 down-regulation in acute gouty arthritis. *Arthritis Res. Ther.* 16: R88.
13. Dai, R., Y. Zhang, D. Khan, B. Heid, D. Caudell, O. Crasta, and S. A. Ahmed. 2010. Identification of a common lupus disease-associated microRNA expression pattern in three different murine models of lupus. *PLoS ONE* 5: e14302. Available at: http://journals.plos.org/plosone/article?id=10.1371/journal.pone.0014302.
14. Wang, G., L. S. Tam, E. K. Li, B. C. Kwan, K. M. Chow, C. C. Luk, P. K. Li, and C. C. Szeto. 2010. Serum and urinary cell-free miR-146a and miR-155 in patients with systemic lupus erythematosus. *J. Rheumatol.* 37: 2516–2522.
15. Wang, G., L. S. Tam, B. C. Kwan, E. K. Li, K. M. Chow, C. C. Luk, P. K. Li, and C. C. Szeto. 2012. Expression of miR-146a and miR-155 in the urinary sediment of systemic lupus erythematosus. *Clin. Rheumatol.* 31: 435–440.
16. Jonsson, R., C. Svalander, and G. Nyberg. 1986. Immune deposits in oral mucosa, skin and kidney in patients with systemic lupus erythematosus. *Clin. Exp. Rheumatol.* 4: 231–236.
17. Andrews, B. S., R. A. Eisenberg, A. N. Theofilopoulos, S. Izui, C. B. Wilson, P. J. McConahey, E. D. Murphy, J. B. Roths, and F. J. Dixon. 1978. Spontaneous murine lupus-like syndromes. Clinical and immunopathological manifestations in several strains. *J. Exp. Med.* 148: 1198–1215.
18. Perkins, D. L., R. M. Glaser, C. A. Mahon, J. Michaelson, and A. Marshak-Rothstein. 1990. Evidence for an intrinsic B cell defect in lpr/lpr mice apparent in neonatal chimeras. *J. Immunol.* 145: 549–555.
19. Dudda, J. C., B. Salaun, Y. Ji, D. C. Palmer, G. C. Monnot, E. Merck, C. Boudousquie, D. T. Utzschneider, T. M. Escobar, R. Perret, et al. 2013. MicroRNA-155 is required for effector $CD8^+$ T cell responses to virus infection and cancer. *Immunity* 38: 742–753.
20. Kong, W., L. He, E. J. Richards, S. Challa, C. X. Xu, J. Permuth-Wey, J. M. Lancaster, D. Coppola, T. A. Sellers, J. Y. Djeu, and J. Q. Cheng. 2014. Upregulation of miRNA-155 promotes tumour angiogenesis by targeting VHL and is associated with poor prognosis and triple-negative breast cancer. *Oncogene* 33: 679–689.
21. O'Connell, R. M., D. Kahn, W. S. Gibson, J. L. Round, R. L. Scholz, A. A. Chaudhuri, M. E. Kahn, D. S. Rao, and D. Baltimore. 2010. MicroRNA-155 promotes autoimmune inflammation by enhancing inflammatory T cell development. *Immunity* 33: 607–619.
22. Kohlhaas, S., O. A. Garden, C. Scudamore, M. Turner, K. Okkenhaug, and E. Vigorito. 2009. Cutting edge: the Foxp3 target miR-155 contributes to the development of regulatory T cells. *J. Immunol.* 182: 2578–2582.
23. Vigorito, E., K. L. Perks, C. Abreu-Goodger, S. Bunting, Z. Xiang, S. Kohlhaas, P. P. Das, E. A. Miska, A. Rodriguez, A. Bradley, et al. 2007. microRNA-155 regulates the generation of immunoglobulin class-switched plasma cells. *Immunity* 27: 847–859.
24. Thai, T. H., H. C. Patterson, D. H. Pham, K. Kis-Toth, D. A. Kaminski, and G. C. Tsokos. 2013. Deletion of microRNA-155 reduces autoantibody responses and alleviates lupus-like disease in the Fas^{lpr} mouse. *Proc. Natl. Acad. Sci. USA* 110: 20194–20199.
25. Lu, L. F., T. H. Thai, D. P. Calado, A. Chaudhry, M. Kubo, K. Tanaka, G. B. Loeb, H. Lee, A. Yoshimura, K. Rajewsky, and A. Y. Rudensky. 2009. Foxp3-dependent microRNA155 confers competitive fitness to regulatory T cells by targeting SOCS1 protein. *Immunity* 30: 80–91.
26. O'Connell, R. M., A. A. Chaudhuri, D. S. Rao, and D. Baltimore. 2009. Inositol phosphatase SHIP1 is a primary target of miR-155. *Proc. Natl. Acad. Sci. USA* 106: 7113–7118.
27. Ceppi, M., P. M. Pereira, I. Dunand-Sauthier, E. Barras, W. Reith, M. A. Santos, and P. Pierre. 2009. MicroRNA-155 modulates the interleukin-1 signaling pathway in activated human monocyte-derived dendritic cells. *Proc. Natl. Acad. Sci. USA* 106: 2735–2740.
28. Galicia-Rosas, G., N. Pikor, J. A. Schwartz, O. Rojas, A. Jian, L. Summers-Deluca, M. Ostrowski, B. Nuesslein-Hildesheim, and J. L. Gommerman. 2012. A sphingosine-1-phosphate receptor 1-directed agonist reduces central nervous system inflammation in a plasmacytoid dendritic cell-dependent manner. *J. Immunol.* 189: 3700–3706.
29. Zhao, C., M. J. Fernandes, M. Turgeon, S. Tancrède, J. Di Battista, P. E. Poubelle, and S. G. Bourgoin. 2008. Specific and overlapping sphingosine-1-phosphate receptor functions in human synoviocytes: impact of TNF-α. *J. Lipid Res.* 49: 2323–2337.
30. Pan, H. F., R. X. Leng, C. C. Feng, X. P. Li, G. M. Chen, B. Z. Li, W. D. Xu, S. G. Zheng, and D. Q. Ye. 2013. Expression profiles of Th17 pathway related genes in human systemic lupus erythematosus. *Mol. Biol. Rep.* 40: 391–399.
31. Brinkmann, V., A. Billich, T. Baumruker, P. Heining, R. Schmouder, G. Francis, S. Aradhye, and P. Burtin. 2010. Fingolimod (FTY720): discovery and development of an oral drug to treat multiple sclerosis. *Nat. Rev. Drug Discov.* 9: 883–897.
32. Spiegel, S., and S. Milstien. 2011. The outs and the ins of sphingosine-1-phosphate in immunity. *Nat. Rev. Immunol.* 11: 403–415.

Supplemental Table I

All the primers used in the experiments are listed below:

PCR primer used for constructing the dual luciferase reporter vector:

S1PR1 3'-UTR-F: CGAGCTCAGACAAGCAAAACAAAGTGAAA

S1PR1 3'-UTR-R: CCCTCGAGTGATAAAGCTATGTGCAAAATG

Real-time PCR primers for detecting the expression of S1PR1 in mouse:

Mus-S1PR1-F: ATGGTGTCCACTAGCATCCC

Mus-S1PR1-R: CGATGTTCAACTTGCCTGTGTAG

Mus-GAPDH-F: AGGTCGGTGTGAACGGATTTG

Mus-GAPDH-R: TGTAGACCATGTAGTTGAGGTCA

Real-time PCR primers for detecting the expression of human and mouse miR-155:

Mus-miR-155RT:

CGCGCCTGCAGGTCGACAATTAACCCTCACTAAAGGGACCCCTATCACAA

Mus-miR-155PCR:

GTAATACGACTCACTATAGGGGAGAAGAGTTAATGCTAATHomo-miR-155RT:

CGCGCCTGCAGGTCGACAATTAACCCTCACTAAAGGGACCCCTATCACGA

Homo-miR-155PCR: GTAATACGACTCACTATAGGGGAGAAGAGTTAATGCTAAT

U6-F: CTCGCTTCGGCAGCACA

U6-R: AACGCTTCACGAATTTGCGT

Real-time PCR primers for detecting the expression of human S1PR1:

Homo-S1PR1-F: AAAGAGCAAACAACTGACCA

Homo-S1PR1-R: GTTAGTCAATTCGTACACATCC

Homo-GAPDH-F: CCAGGTGGTCTCCTCTGACTT

Homo-GAPDH-R: GTTGCTGTAGCCAAATTCGTTGT

Real-time PCR primers for verification of microarray chip results:

Satb1-F: TTCAGTTACACAGTTGCCCT

Satb1-R: CTATCCATCTCAACCATCATATCC

Malt1-F: GGCGTTCACATTCAATTAGG

Malt1-R: ATCTAGGTCAAGAGGGAAATCAG

Pxk-F: CATCCGGGTGCAAAGAGGAAT

Pxk-R: CTCACGGTCCATGTTTCCAAT

Cbfb-F: CACAGATTGGATGGTATGGG

Cbfb-R: TCTTCTTGCCTCCATTTCCA

Sla-F: ATTATCGAATCTTCCGTCTTCC

Sla-R: CAGCCACTTCAGAATAATGAG

Traf4-F: GTGCCTACTGTACCAAGGAATTT

Traf4-R: AGATGTGGCTTTACGCTCTCC

Cxcr5-F: ATATGGATGACCTGTACAAGGA

Cxcr5-R: AAGGCAGGATGAAGACTAAGAG

Cr2-F: GTTACTTGCTCAACTTTGACC

Cr2-R: TAACTGGAACCCTTCATCAC